



Universiteit
Leiden
The Netherlands

Detection of interstellar H₂D⁺ emission

Stark, R.; Tak, F.F.S. van der; Dishoeck, E.F. van

Citation

Stark, R., Tak, F. F. S. van der, & Dishoeck, E. F. van. (1999). Detection of interstellar H₂D⁺ emission. Retrieved from <https://hdl.handle.net/1887/2282>

Version: Not Applicable (or Unknown)

License: [Leiden University Non-exclusive license](#)

Downloaded from: <https://hdl.handle.net/1887/2282>

Note: To cite this publication please use the final published version (if applicable).

DETECTION OF INTERSTELLAR H₂D⁺ EMISSION

RONALD STARK

Max-Planck-Institut für Radioastronomie, Auf dem Hügel 69, D-53121 Bonn, Germany

AND

FLORIS F. S. VAN DER TAK AND EWINE F. VAN DISHOCK

Sterrewacht Leiden, Postbus 9513, NL-2300 RA Leiden, The Netherlands

Received 1999 May 10; accepted 1999 June 11; published 1999 July 15

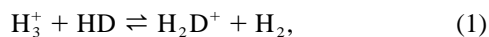
ABSTRACT

We report the detection of the $1_{10-1_{11}}$ ground-state transition of ortho-H₂D⁺ at 372.421 GHz in emission from the young stellar object NGC 1333 IRAS 4A. Detailed excitation models with a power-law temperature and density structure yield a beam-averaged H₂D⁺ abundance of 3×10^{-12} with an uncertainty of a factor of 2. The line was not detected toward W33A, GL 2591, and NGC 2264 IRS (in the latter source at a level that is 3–8 times lower than previous observations). The H₂D⁺ data provide direct evidence in support of low-temperature chemical models in which H₂D⁺ is enhanced by the reaction of H₃⁺ and HD. The H₂D⁺ enhancement toward NGC 1333 IRAS 4A is also reflected in the high DCO⁺/HCO⁺ abundance ratio. Simultaneous observations of the N₂H⁺ 4–3 line show that its abundance is about 50–100 times lower in NGC 1333 IRAS 4A than in the other sources, suggesting significant depletion of N₂. The N₂H⁺ data provide independent lower limits on the H₃⁺ abundance that are consistent with the abundances derived from H₂D⁺. The corresponding limits on the H₃⁺ column density agree with recent near-infrared absorption measurements of H₃⁺ toward W33A and GL 2591.

Subject headings: ISM: abundances — ISM: molecules — molecular processes — radio lines: ISM — submillimeter

1. INTRODUCTION

The recent detection of the H₃⁺ ion in interstellar clouds through its infrared vibration-rotation lines (Geballe & Oka 1996; McCall et al. 1998) is an important confirmation of the gas-phase chemical networks (Herbst & Klemperer 1973; Watson 1973b). Because of its symmetry, H₃⁺ has no allowed rotational transitions contrary to its deuterated isotopomer H₂D⁺, which has a large permanent dipole moment (Dalgarno et al. 1973). Thus, H₂D⁺ is important as a tracer of H₃⁺ with transitions that can be searched for in emission. In addition, it is widely believed to play a pivotal role in the interstellar ion-molecule chemistry at low temperatures where significant enhancement of deuterated molecules occurs as a result of fractionation (e.g., Watson 1973a; Herbst 1982; Millar, Bennett, & Herbst 1989). This process is initiated by the isotope exchange equilibrium reaction



which is shifted in the forward direction at low temperatures (Smith, Adams, & Alge 1982; Herbst 1982). The formation of H₂D⁺ is followed by deuterium transfer reactions with, e.g., CO to form DCO⁺, and the H₂D⁺ enhancement is reflected in the observed large abundance ratios of, e.g., DCO⁺/HCO⁺, NH₂D/NH₃, and DCN/HCN in cold clouds (e.g., Wootten 1987; Butner, Lada, & Loren 1995; Williams et al. 1998).

Over the last 20 years, numerous attempts have been made to detect the $1_{10-1_{11}}$ ortho-H₂D⁺ and $1_{01-0_{00}}$ para-H₂D⁺ ground-state lines at 372 and 1370 GHz, respectively. These searches have mainly been done with the Kuiper Airborne Observatory (KAO) (Phillips et al. 1985; Pagani et al. 1992b; Boreiko & Betz 1993), and a possible absorption feature at 1370 GHz has been reported by Boreiko & Betz (1993) toward Orion. Observations from the ground are very difficult since the 372 GHz line is at the edge of a strong atmospheric water absorption line, while the atmosphere at 1370 GHz is almost completely

opaque. With the advent of new submillimeter receivers equipped with sensitive niobium SIS mixers, it has become possible to search for weak ortho-H₂D⁺ lines from high, dry sites such as Mauna Kea. Indeed, a ground-based search for this line from the Caltech Submillimeter Observatory by van Dishoeck et al. (1992) yielded limits that are up to a factor of 100 more sensitive than those obtained with the KAO. Comparison with chemical models suggested that only a factor of a few improvement would be needed to detect the line. With the new facility receiver RxB3 at the James Clerk Maxwell Telescope (JCMT),¹ such an improvement in sensitivity is now achievable. Here we report the detection of the H₂D⁺ 372.421 GHz line toward NGC 1333 IRAS 4A and significant upper limits toward W33A, GL 2591, and NGC 2264 IRS. Simultaneous observations of the N₂H⁺ 4–3 line at 372.672 GHz toward these young stellar objects (YSOs) are used to place additional constraints on the H₃⁺ abundance.

2. OBSERVATIONS

The observations of the $1_{10-1_{11}}$ ground-state transition of ortho-H₂D⁺ at 372.42134 GHz (Bogey et al. 1984) were done with the JCMT in 1998 August 31 and September 15 and 18 during three nights of very good submillimeter transparency with a zenith opacity at 225 GHz below 0.05. The dual-polarization heterodyne receiver RxB3 was used.² Both mixers were tuned to 372.5469 GHz in the upper sideband. The big advantage of RxB3 is that it has a dual-beam interferometer that allows single-sideband (SSB) operation, enhancing the sensitivity and calibration at 372 GHz considerably. The digital autocorrelator spectrometer was split into four parts of

¹ The JCMT is operated by the Joint Astronomy Centre (JAC) in Hilo, Hawaii, on behalf of the Particle Physics and Astronomy Research Council in the UK, the Netherlands Organisation for Scientific Research, and the National Research Council of Canada.

² The junctions for the RxB3 mixers were fabricated by SRON/DIMES.

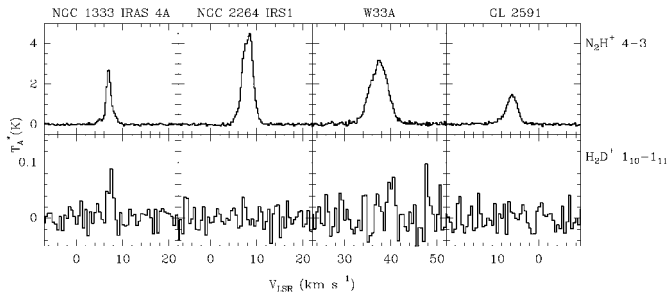


FIG. 1.—Observed spectra of H₂D⁺ 1₁₀–1₁₁ at 372.421 GHz and N₂H⁺ 4–3 at 372.672 GHz. The N₂H⁺ spectra have a resolution of 0.3 km s^{−1}. The H₂D⁺ spectra have been smoothed to 0.6 km s^{−1}.

125 MHz. This setup allows observations of both lines in two orthogonal polarizations simultaneously, with a spectral resolution of 376 kHz ($\equiv 0.3$ km s^{−1} at 372 GHz). Typical SSB system temperatures, including atmospheric losses, were about 1200 K. The effective total integration time was 7 hr on NGC 1333 observed over two nights, 2.7 hr on W33A, 4.3 hr on GL 2591, and 4 hr on NGC 2264. The absolute calibration uncertainty is estimated at 30%, and the relative calibration between the H₂D⁺ and N₂H⁺ lines is much better. The JCMT beam size at 372 GHz is 13" FWHM; the main-beam efficiency is 57%. JCMT data on H¹³CO⁺ and DCO⁺ were taken from the literature (see below), except for DCO⁺ toward W33A and GL 2591, for which the 3–2 transition at 216.113 GHz was observed with receiver RxA3. The beam size at this frequency is 21" FWHM, and the main-beam efficiency is 70%.

The observed H₂D⁺ and N₂H⁺ spectra are presented in Figure 1. The source and line parameters are listed in Table 1. The H₂D⁺ line is clearly detected with $T_A^* = 0.08 \pm 0.03$ K toward NGC 1333 IRAS 4A and is seen in spectra of both nights. The velocity width shows good agreement with the N₂H⁺ line width, while the velocities are offset by about 0.5 km s^{−1}. Comparison with the line survey of Blake et al. (1995) shows that such an offset is small and common for this region.

No H₂D⁺ emission was detected toward NGC 2264 IRS, W33A, and GL 2591. Assuming the same width as the N₂H⁺ line, 2 σ upper limits of $T_A^* \leq 0.02$ –0.04 K are obtained. For NGC 2264, this limit is about a factor of 8 below the possible feature of Phillips et al. (1985) and a factor of 3 below the limit reached by van Dishoeck et al. (1992). Note that the N₂H⁺

emission toward NGC 1333 is much weaker than that toward the other sources. No other lines were detected in the 125 MHz bands.

3. ANALYSIS

Model calculations were performed to determine the abundances of H₂D⁺, N₂H⁺, HCO⁺, and DCO⁺ using a power-law density structure $n = n_0(r/R_o)^{-\alpha}$, as described in van der Tak et al. (1999a). In these models, the radial dust temperature profile is calculated from the observed luminosity, and n_0 is determined from submillimeter photometry, which probes the total dust mass. The grain heating and cooling are solved self-consistently as a function of radius, r , using grain properties from Ossenkopf & Henning (1994). The outer radius (R_o) is determined from high-resolution submillimeter line and continuum maps. The exponent α is constrained by modeling the relative strength of emission lines of CS and H₂CO at the central position over a large range of critical densities with a Monte Carlo radiative transfer program, assuming $T_K = T_{\text{dust}}$. Data were taken from Blake et al. (1995) (NGC 1333 IRAS 4A), de Boisanger, Helmich, & van Dishoeck (1996) and Schreyer et al. (1997) (NGC 2264 IRS), and van der Tak et al. (1999a, 1999b) (GL 2591 and W33A). For NGC 1333 IRAS 4A, where CS is heavily depleted, $\alpha = 2$ was taken based on the analysis of the continuum visibilities in interferometer data by Looney (1998).

Given the calculated temperature and density structure, the radiative transfer models were run in order to determine the abundances, assuming initially a constant abundance throughout the envelope. Both the ortho-H₂D⁺ and para-H₂D⁺ ladders have been considered since their spin states are coupled through reactive collisions with H₂; thus, the para 0₀₀ level is the true rotational ground state. A de-excitation rate coefficient of 1.0×10^{-10} cm³ s^{−1} has been used for all inter-ladder transitions (see Herbst 1982 and Pagani, Salez, & Wannier 1992a for a detailed study of the ortho/para ratio). The lower level of the 1₁₀–1₁₁ transition lies at 86 K. The excitation energy of the 1₁₀ level is 18 K relative to the 1₁₁ level, and the critical density for this transition is about 2×10^5 cm^{−3}.

The calculated abundances are listed in Table 2. Toward NGC 1333, we infer a beam-averaged abundance $x(\text{H}_2\text{D}^+) = 3 \times 10^{-12}$. Upper limits on the abundance toward NGC 2264, W33A, and GL 2591 are less than 1×10^{-11} . The N₂H⁺ abundance ranges between 10^{-11} toward NGC 1333 and 10^{-9} toward

TABLE 1
OBSERVATIONS^a

Source ^b	Molecule	Transition	T_A^* (K)	ΔV (km s ^{−1})	V_{LSR} (km s ^{−1})
N1333	H ₂ D ⁺	1 ₁₀ –1 ₁₁	0.08 (0.03)	1.2 \pm 0.3	7.4 \pm 0.2
	N ₂ H ⁺	4–3	2.57 (0.03)	1.35	6.94
N2264	H ₂ D ⁺	1 ₁₀ –1 ₁₁	$\leq 0.02^c$
	N ₂ H ⁺	4–3	4.51 (0.03)	2.67	8.01
W33A	H ₂ D ⁺	1 ₁₀ –1 ₁₁	$\leq 0.04^c$
	N ₂ H ⁺	4–3	3.06 (0.06)	4.62	37.40
GL 2591	H ₂ D ⁺	1 ₁₀ –1 ₁₁	$\leq 0.02^c$
	N ₂ H ⁺	4–3	1.41(0.04)	2.89	−5.82

^a The values in parentheses represent 1 σ statistical uncertainties. The absolute uncertainty of the intensity is 30%; ΔV and V_{LSR} are accurate to better than 0.1 km s^{−1}.

^b Position (B1950): NGC 1333 IRAS 4A ($\alpha = 03^{\text{h}}26^{\text{m}}04^{\text{s}}.8$, $\delta = +31^{\circ}03'14''$); NGC 2264 IRS ($\alpha = 06^{\text{h}}38^{\text{m}}25^{\text{s}}.0$, $\delta = +09^{\circ}32'29''$); W33A ($\alpha = 18^{\text{h}}11^{\text{m}}44^{\text{s}}.2$, $\delta = -17^{\circ}52'56''$); and GL 2591 ($\alpha = 20^{\text{h}}27^{\text{m}}35^{\text{s}}.8$; $\delta = +40^{\circ}01'14''$).

^c The 2 σ limits: NGC 2264 IRS ($\Delta V = 2.5$ km s^{−1}), GL 2591 ($\Delta V = 3.0$ km s^{−1}), and W33A ($\Delta V = 4.5$ km s^{−1}).

TABLE 2
EXCITATION MODEL PARAMETERS AND DEDUCED ABUNDANCES^a

SOURCE	α	n_0 (cm^{-3})	T (K)		MOLECULAR ABUNDANCES							
			R_i	R_o	H_2D^+	N_2H^+	H_3^+ ^b	H_3^{c}	$\text{H}_2\text{D}^+/\text{H}_3^+$	$\text{DCO}^+/\text{HCO}^+$ ^d	CO^e	N_2
N1333	2	1.7(6)	318	13	3(-12)	1(-11)	2(-10)	>2(-11)	2(-2)	1(-2)	4(-6)	4(-7)
N2264	1.5	1.5(4)	293	18	<1(-11)	6(-10)	<3(-9)	>1(-9)	<3(-3)	3(-3)	6(-5)	4(-5)
W33A	1	2.1(4)	280	16	<1(-11)	1(-9)	<4(-9)	>2(-9)	<3(-3)	1(-4)	5(-5)	2(-5)
GL 2591	1.25	3.5(4)	350	30	<1(-11)	5(-10)	<3(-9)	>1(-9)	<3(-3)	4(-4)	2(-4)	9(-5)

^a From statistical equilibrium calculations using the appropriate temperature and density structure as a function of distance r to the YSO, $n(r) = n_o(r/R_o)^{-\alpha}$, where R_o is the outer radius of the model envelope: NGC 1333 IRAS 4A [3.1(3) AU], NGC 2264 IRS [4.7(4) AU], W33A [2.4(5) AU], GL 2591 [3.1(4) AU], and $R_i = R_o/300$ is the inner radius. The notation $a(b)$ indicates $a \times 10^b$. The accuracy of the deduced abundances is a factor of 2.

^b From H_2D^+ using a theoretical $\text{H}_3^+/\text{H}_2\text{D}^+$ ratio at the effective temperature from which most of the emission arises (see Fig. 2).

^c From N_2H^+ analysis (see text).

^d From H^{13}CO^+ assuming $\text{HCO}^+/\text{H}^{13}\text{CO}^+ = 60$.

^e From C^{17}O assuming $\text{CO}/\text{C}^{17}\text{O} = 2500$ and using the appropriate $N(\text{H}_2)$ from submillimeter dust emission in a 13" beam: NGC 1333 IRAS 4A [$3.1(23) \text{ cm}^{-2}$], NGC 2264 IRS [$1.2(23) \text{ cm}^{-2}$], W33A [$5.2(23) \text{ cm}^{-2}$], and GL 2591 [$1.3(23) \text{ cm}^{-2}$].

W33A. All derived abundances have an absolute uncertainty of a factor of 2 because of the uncertainties in the dust opacities and CO abundances. The relatively high N_2H^+ abundance toward NGC 2264 was already found by van Dishoeck et al. (1992), who noted that nearly all of the gas-phase nitrogen must be in the form of N_2 in this cloud. Since N_2H^+ is formed mainly by the reaction of H_3^+ and N_2 , the latter observations provide an independent lower limit on the H_3^+ abundance. Destruction occurs mainly via reactions with CO, O, and electrons. Considering CO destruction only,

$$n(\text{H}_3^+) \geq 0.5n(\text{N}_2\text{H}^+)x(\text{CO})/x(\text{N}_2). \quad (2)$$

Assuming 50% of the nitrogen is in N_2 , $x(\text{N}_2) = 5 \times 10^{-5}\delta(\text{N}_2)$, $x(\text{CO}) = 2 \times 10^{-4}\delta(\text{CO})$, and equal amounts of depletion δ for CO and N_2 , this yields $x(\text{H}_3^+) \geq 2x(\text{N}_2\text{H}^+)$. These limits are listed in Table 2 and are consistent with the upper limits derived from the H_2D^+ observations using a theoretical $\text{H}_2\text{D}^+/\text{H}_3^+$ ratio (see § 4).

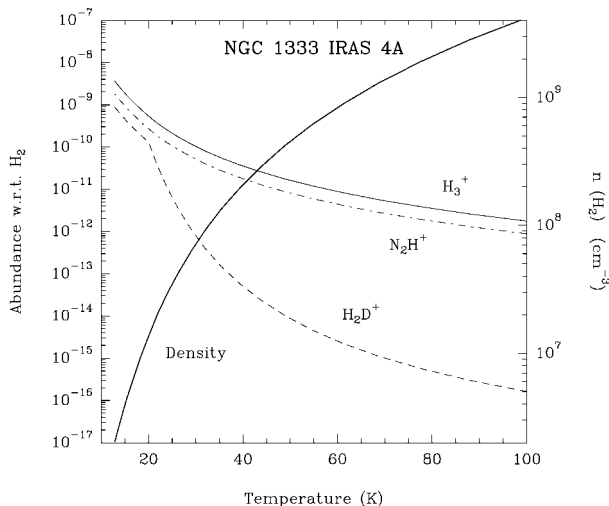
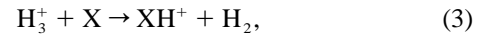


FIG. 2.—Power-law model abundances of H_3^+ , H_2D^+ , and N_2H^+ as a function of density and temperature.

4. $\text{H}_2\text{D}^+/\text{H}_3^+$ CHEMISTRY

The above analysis assumes constant abundances throughout the YSO envelopes. In reality, the H_2D^+ abundance is a strong function of temperature and position. In chemical equilibrium, the H_3^+ abundance can be written as $x(\text{H}_3^+) = \zeta/\sum k_x n(\text{X})$, with $n(\text{X}) = n(\text{H}_2)x(\text{X})$. X refers to any of O, C, CO, O_2 , N_2 , H_2O , etc., which are the principal removal agents of H_3^+ via the proton transfer reactions



where k_x are the rate coefficients (taken from the UMIST database; see, e.g., Millar, Farquhar, & Willacy 1997) and ζ is the cosmic-ray ionization rate (taken to be $5 \times 10^{-17} \text{ s}^{-1}$). A simple chemical model for the formation and destruction of H_2D^+ yields

$$\frac{x(\text{H}_2\text{D}^+)}{x(\text{H}_3^+)} = \frac{x(\text{HD})k_f + x(\text{D})k_D}{x(e)k_e + \sum k_x x(\text{X}) + k_r}, \quad (4)$$

where k_f and k_r are the forward and backward rate coefficients of reaction (1), k_D is the rate coefficient for the formation of H_2D^+ through the reaction $\text{H}_3^+ + \text{D}$, and k_e is the rate coefficient of the electron recombination of H_2D^+ (see, e.g., Caselli et al. 1998 for a compilation of values). We assumed $x(\text{HD}) = 10x(\text{D}) = 2.8 \times 10^{-5}$ throughout.

The above H_3^+ and H_2D^+ chemical equations were included in the power-law models, and abundances at each position were calculated for the appropriate temperature and density. We have fixed the expression for k_r at $T < 20$ K to its value at 20 K, to ensure that $x(\text{H}_2\text{D}^+) < x(\text{H}_3^+)$ throughout. For simplicity, only $\text{X} = \text{CO}$ was considered, and the electron recombination was neglected. The CO depletions are inferred from C^{17}O observations using the method described by van der Tak et al. (1999a, 1999b) and are listed in Table 2. For a homogeneous temperature and density structure, our model agrees well with the models of Millar et al. (1989) and Pagani et al. (1992a).

The power-law model results for NGC 1333 IRAS 4A are presented in Figure 2. Using these abundances, the H_2D^+ emission has been calculated, most of which originates from gas at $T = 25\text{--}35$ K. The model intensity agrees within 30% with that measured toward NGC 1333 IRAS 4A and is consistent with the upper limit toward GL 2591. They are a factor of 2 and 4 larger than the upper limits toward NGC 2264 IRS and

W33A, respectively. Most likely, this small discrepancy results from the effective removal of H₃⁺ by other species than CO and/or by an overestimate of the size of the cloud. The H₃⁺ column densities computed for W33A and GL 2591 agree within a factor of 2–3 with the directly observed column densities by Geballe & Oka (1996) and McCall et al. (1998). This good agreement between models and observations provides the strongest support for the basic H₃⁺ and H₂D⁺ chemical networks in dense, cold clouds.

The simple chemical networks described above (eq. [2] and reaction [3]) have also been used to model the N₂H⁺ abundance from the N₂H⁺/H₂D⁺ ratio. Assuming equal amounts of depletion for CO and N₂, agreement within a factor of 2 between the measured and modeled N₂H⁺ line intensities is obtained. The best-fitting N₂ abundances are included in Table 2.

The derived H₂D⁺/H₃⁺ ratios are also compared with the observed DCO⁺/HCO⁺ ratios in Table 2. The enhancement in H₂D⁺/H₃⁺ is clearly reflected in the DCO⁺/HCO⁺ ratio, as expected, since the latter species are directly formed by reactions of the former with CO. For NGC 1333 IRAS 4A, DCO⁺/HCO⁺ = 0.5H₂D⁺/H₃⁺, where the factor of 0.5 is consistent with the statistical branching ratio of 1/3 within the uncertainties. The DCO⁺/HCO⁺ ratio toward NGC 1333 IRAS 4A is a factor of 5–50 higher than that toward the other sources. This can be explained by the difference in physical structure. In cold, dense (pre)protostellar cores like NGC 1333 IRAS 4A where the CO and N₂ depletions are extreme, the H₂D⁺ abundance is enhanced, because of the low temperature and because the main removal reactions of H₃⁺ are suppressed. The H₂D⁺ abundance will increase even stronger than that of H₃⁺ since reaction (1) becomes the main destruction channel of H₃⁺. In the case of NGC 2264, W33A, and GL 2591, where the temperatures are higher and the depletion of CO and N₂ is less, reaction (3) becomes the main removal path of H₃⁺.

The difference in physical structure may have its origin in the different stages of protostellar evolution. In particular, NGC 1333 IRAS 4A has been classified as a class 0 object (André & Montmerle 1994) and is thus in a very early stage, with a large spatial separation between the quiescent and shocked regions (Blake et al. 1995).

5. CONCLUSIONS

With the current sensitivity of heterodyne receivers, it is now possible to study the ortho-H₂D⁺ 1₁₀–1₁₁ 372.421 GHz line profile in emission in the early stages of star formation deep inside dense molecular clouds. Its importance lies in the fact that it is a tracer of H₃⁺ and that it provides information on the deuterium abundance and temperature history of a cloud and on the chemical evolution during star formation. Further observations of the H₂D⁺ and H₃⁺ lines in a sample of very young class 0 and class I YSOs will therefore be very valuable.

Since the ortho-H₂D⁺ ground state is at 86 K, the 1₁₀–1₁₁ line traces both the warm and cold regions, although the H₂D⁺ enhancement will be strongest in the coldest regions. Observations of the 1₀₁–0₀₀ para-H₂D⁺ ground-state line at 1.37 THz toward the continuum of embedded YSOs may reveal cold H₂D⁺ in absorption. The dual-channel German REceiver for Astronomy at Terahertz frequencies (GREAT), to be flown on the Stratospheric Observatory For Infrared Astronomy (SOFIA), would allow such observations. Combined with 372 GHz observations from the ground, the total abundance and the relative population of the ortho- and para-modifications may be determined, and this would provide information on the formation, destruction, and excitation processes. Simultaneous deep observations of the HD *J* = 1–0 (2.7 THz) and para-H₂D⁺ ground-state lines toward YSOs may yield a direct measure of the (variation in) H₃⁺ abundance over the cloud and thus of the cosmic-ray ionization rate.

It is a pleasure to thank Lorne Avery for discussions and test observations at 372 GHz, Henry Matthews for the non-standard setup for the back end, and Leslie Looney and Lee Mundy for sharing their model results on NGC 1333 prior to publication. The observations would not have been possible without the flexible observing strategy of Remo Tilanus. Gerd-Jan van Zadelhoff, Fred Baas, and Jane Greaves did an excellent job in carrying out these observations in service. This work is supported by NWO grant 614.41.003.

REFERENCES

- André, P., & Montmerle, T. 1994, *ApJ*, 420, 837
 Blake, G. A., Sandell, G., van Dishoeck, E. F., Groesbeck, T. D., Mundy, L. G., & Aspin, C. 1995, *ApJ*, 441, 689
 Bogey, M., Demuynck, C., Denis, M., Destombes, J. L., & Lemoine, B. 1984, *A&A*, 137, L15
 Boreiko, R. T., & Betz, A. L. 1993, *ApJ*, 405, L39
 Butner, H. M., Lada, E. A., & Loren, R. B. 1995, *ApJ*, 448, 207
 Caselli, P., Walmsley, C. M., Terzieva, R., & Herbst, E. 1998, *ApJ*, 499, 234
 Dalgarno, A., Herbst, E., Novick, S., & Klemperer, W. 1973, *ApJ*, 183, L131
 de Boisanger, C., Helmich F. P., & van Dishoeck, E. F. 1996, *A&A*, 310, 315
 Geballe, T. R., & Oka, T. 1996, *Nature*, 384, 334
 Herbst, E. 1982, *A&A*, 111, 76
 Herbst, E., & Klemperer, W. 1973, *ApJ*, 185, 505
 Looney, L. 1998, Ph.D. thesis, Univ. Maryland
 McCall, B. J., Hinkle, K. H., Geballe, T. R., & Oka, T. 1998, *Faraday Discuss.*, 109, 267
 Millar, T. J., Bennett, A., & Herbst, E. 1989, *ApJ*, 340, 906
 Millar, T. J., Farquhar, P. R. A., & Willacy, K. 1997, *A&AS*, 121, 139
 Ossenkopf, V., & Henning, Th. 1994, *A&A*, 291, 943
 Pagani L., Salez, M., & Wannier, P. G. 1992a, *A&A*, 258, 479
 Pagani, L., et al. 1992b, *A&A*, 258, 472
 Phillips, T. G., Blake, G. A., Keene, J., Woods, R. C., & Churchwell, E. 1985, *ApJ*, 294, L45
 Schreyer, K., Helmich, F. P., van Dishoeck, E. F., & Henning, Th. 1997, *A&A*, 326, 347
 Smith, D., Adams, N. G., & Alge, E. 1982, *ApJ*, 263, 123
 van der Tak, F. F. S., van Dishoeck E. F., Evans, N. J., II, Bakker, E. J., & Blake, G. A. 1999a, *ApJ*, in press
 van der Tak, F. F. S., van Dishoeck E. F., Evans, N. J., II, & Blake, G. A. 1999b, in preparation
 van Dishoeck, E. F., Phillips, T. G., Keene, J., & Blake, G. A. 1992, *A&A*, 261, L13
 Watson, W. D. 1973a, *ApJ*, 182, L73
 ———. 1973b, *ApJ*, 183, L17
 Williams, J. P., Bergin, E. A., Caselli, P., Myers, P. C., & Plume, R. 1998, *ApJ*, 503, 689
 Wootten, A. 1987, in *IAU Symp. 120, Astrochemistry*, ed. M. S. Vardya & S. P. Tarafdar (Dordrecht: Kluwer), 311